

# Empirical Mode Decomposition for Trivariate Signals

Naveed ur Rehman, *Student Member, IEEE*, and Danilo P. Mandic, *Senior Member, IEEE*

**Abstract**—An extension of empirical mode decomposition (EMD) is proposed in order to make it suitable for operation on trivariate signals. Estimation of local mean envelope of the input signal, a critical step in EMD, is performed by taking projections along multiple directions in three-dimensional spaces using the rotation property of quaternions. The proposed algorithm thus extracts rotating components embedded within the signal and performs accurate time-frequency analysis, via the Hilbert–Huang transform. Simulations on synthetic trivariate point processes and real-world three-dimensional signals support the analysis.

**Index Terms**—Empirical mode decomposition (EMD), Hilbert–Huang spectrum, motion analysis, quaternion algebra, rotation property of quaternions, spiking neurons, time-frequency analysis, trivariate signals, wind modeling.

## I. INTRODUCTION

THE empirical mode decomposition (EMD) algorithm has been designed for the time-frequency analysis of real-world signals [1]. It decomposes the signal in hand into a number of oscillatory modes called intrinsic mode functions (IMFs), so that the application of Hilbert transform to these intrinsic mode functions provides meaningful instantaneous frequency estimates [2]. The IMFs are obtained directly from the data with no *a priori* assumptions regarding the data nature, making EMD suitable for the analysis of nonlinear and nonstationary signals. The time-frequency analysis via EMD has found a wide range of applications in signal processing and related fields [3]–[5].

The original EMD algorithm has been designed to process real-valued data, whereas for the processing of bivariate signals, several algorithms for complex EMD have been proposed [6]. The complex EMD algorithm [7] proposed by Tanaka and Mandic effectively applies real-valued EMD to the signals corresponding to the positive and negative frequency component of the spectrum of analytic signals. The rotation-invariant complex EMD (RI-EMD) [8] extends the real-valued EMD to the complex (bivariate) domain in a generic way. Since all the operations are performed directly in  $\mathbb{C}$ , this method provides a single set of complex IMFs. An extension of RI-EMD developed by Rilling *et al.*, also termed the bivariate EMD [9], separates “fast rotating” components of a complex signal from “slowly rotating” ones. Envelope curves are obtained by projecting a bi-

variate signal in multiple directions and interpolating their extrema. The local mean is calculated by averaging the envelope curves and is then subtracted from the original signal repeatedly to sift out rotating components within the signal. Recently, complex extensions of EMD have found applications in data fusion [10] from multiple and heterogenous sources, due to their ability to extract common oscillating modes of each component (real and imaginary) of a bivariate signal, in the corresponding complex IMFs [11]. In addition to the extensions of EMD to complex (bivariate) time series, various methods have been developed to generalize EMD to process two-dimensional (2D) signals, which have found applications in the processing of 2D images [12], [13]. At present, the applications of EMD are limited to real-valued, complex (bivariate), and 2D signals, and its further extensions are a prerequisite to data-driven time-frequency analysis of trivariate and three-dimensional (3D) signals.

The proposed extension of EMD operates on trivariate signals and considers a trivariate signal as a pure quaternion, with each of its component a real-valued time series, such as 3D wind data, multichannel EEG (Electroencephalogram) signals, and 3D inertial sensor (accelerometer and gyroscope) data. The processing of trivariate time series directly in a 3D space yields better results than using multiple univariate models applied to each component separately. This is demonstrated by the ability of the proposed method to generate common modes of the input signal in each quaternion-valued IMF. The alignment of common modes is achieved because the proposed method is designed to process a trivariate signal under the umbrella of quaternion calculus. As a result, the method is expected to find applications in data fusion from multiple sources.

The proposed method uses the quaternion rotation framework [14], [15] to take projections of the input signal in multiple directions in a 3D space in order to calculate the mean envelope curve of a trivariate signal. Quaternions are preferred over other methods for 3D rotations, such as Euler’s angle and rotation matrices, as they offer more compact notation, less computational demands, better accuracy, intuitive representation of rotation in terms of the rotation axis and angle, and their use helps to avoid the singularity problems associated with Euler angles. Their recent applications have been in the modeling of 3D rotations [16], [17], adaptive filtering [18], [19], gait analysis [20], and robotics [21].

The organization of this paper is as follows: Section II describes the real-valued EMD and its bivariate (complex) extensions, Section III gives a brief overview of quaternion algebra, Section IV introduces the proposed algorithm, and Section V presents simulation results and discussion.

## II. REAL-VALUED EMD AND ITS BIVARIATE EXTENSIONS

Real-valued EMD [1] aims to adaptively decompose a signal into a finite set of oscillatory components called “intrinsic mode

Manuscript received January 28, 2009; accepted September 01, 2009. First published October 06, 2009; current version published February 10, 2010. The associate editor coordinating the review of this manuscript and approving it for publication was Prof. Cédric Richard.

The authors are with the Department of Electrical and Electronic Engineering, Imperial College London, London SW7 2AZ, U.K. (e-mail: naveed.rehman07@imperial.ac.uk; d.mandic@ic.ac.uk).

Color versions of one or more of the figures in this paper are available online at <http://ieeexplore.ieee.org>.

Digital Object Identifier 10.1109/TSP.2009.2033730

functions” (IMFs). This is achieved by sifting out rapidly oscillating components (dominant modes) from the data, by iteratively subtracting less dominant modes (slowly oscillating components). These slowly oscillating components are defined as the local mean of a signal. Once extracted, an IMF has the local mean value of zero, and the sifting process is stopped when all the dominant modes are extracted. More specifically, if  $x(k)$  denotes a real-valued input signal, then the application of EMD yields a set of  $M$  IMFs, denoted by  $\{d_j(k)\}_{j=1}^M$ , such that

$$x(k) = \sum_{j=1}^M d_j(k) + r(k) \quad (1)$$

where the residual  $r(k)$  is a monotonic function and represents the trend within the original signal. In order to obtain physically meaningful instantaneous frequency estimates, the IMFs should be designed so as to be symmetric around the local mean, and their number of extrema and zero crossings should differ at most by one [1]. This requirement ensures that the IMFs have no positive local minima and no negative local maxima. The procedure used for the extraction of an IMF from a signal  $x'(k)$  is given in Algorithm 1.

---

#### Algorithm 1 Empirical Mode Decomposition

---

- 1: Find the locations of all the extrema of  $x'(k)$ .
  - 2: Interpolate (using spline interpolation) between all the minima (resp. maxima) to obtain the signal envelope passing through the minima,  $e_{\min}(k)$  (resp.  $e_{\max}(k)$ ).
  - 3: Compute the local mean  $m(k) = (e_{\min}(k) + e_{\max}(k)) / 2$ .
  - 4: Subtract the mean from the signal to obtain the “oscillating” signal  $s(k) = x'(k) - m(k)$ .
  - 5: If the resulting signal  $s(k)$  obeys the stopping criterion,  $d(k) = s(k)$  becomes an IMF; otherwise set  $x'(k) = s(k)$  and repeat the process from Step 1.
- 

The stoppage criterion used in the final step can be, for instance, the normalized squared difference between two successive sifting iterates  $s_n(k)$  and  $s_{n-1}(k)$ , that is

$$\sum_{k=0}^N \frac{\|s_{n-1}(k) - s_n(k)\|^2}{s_{n-1}^2(k)} \leq SD \quad (2)$$

where  $N$  represents the total number of samples in the original series  $x(k)$ , and the empirical value of  $SD$  is usually set within the range (0.2–0.3). However, this criterion does not depend on the actual definition of IMF and may underperform in practice. A more robust criterion, based on the original definition of IMF, stops the sifting process only after the condition on the extrema of an IMF is met for  $S$  consecutive iterations [22]. It has also been shown in [22] that the empirical range of  $S$  should be chosen between 4 and 8.

Upon obtaining an IMF, the next IMF is extracted by applying the same procedure to the residual signal  $r(k) = x'(k) - d(k)$ . The process is repeated until all the IMFs are extracted and the remaining signal carries no more oscillations, characterized by an inadequate number of extrema. The application of the Hilbert

transform to the set of IMFs yields physically meaningful instantaneous frequency and amplitude information and provides a convenient time-frequency-energy description of a time-series in the form of Hilbert–Huang spectrum [2].

#### A. Bivariate (Complex) Extensions of EMD

Recently, several extensions of EMD have been proposed to make it suitable for the operation on bivariate (complex) signals. The complex EMD [7] makes use of the analyticity of the signal to apply the real-valued EMD [1] component-wise, whereas RI-EMD [8] and bivariate EMD [9] estimate the local mean based on the envelopes obtained by taking projections of the input signal in different directions.

1) *Complex EMD*: For bivariate signals, complex EMD [7] uses the positive and negative frequency components to apply standard EMD to two real-valued time series. This is achieved by converting a general nonanalytic signal into two analytic signals, each corresponding to either the positive or the negative frequency components of the original signal. The standard EMD is then applied to the real part of the resulting analytic signals to obtain two sets of IMFs. These sets of IMFs are then combined to form complex-valued IMFs.

More precisely, let  $x[n]$  be a complex-valued sequence and  $X(e^{j\omega})$  its discrete Fourier transform. By processing signal  $x[n]$  with the filter with the transfer function

$$H(e^{j\omega}) = \begin{cases} 1, & 0 < \omega \leq \pi \\ 0, & -\pi < \omega \leq 0 \end{cases} \quad (3)$$

the digital Fourier transform (DFT) of two analytic signals, denoted by  $X_+(e^{j\omega})$  and  $X_-(e^{j\omega})$ , are generated, which correspond respectively to the positive and the negative frequency parts of  $X(e^{j\omega})$ . The subsequent application of the inverse Fourier transform, denoted by  $\mathcal{F}^{-1}[\cdot]$ , yields time series  $x_+[n]$  and  $x_-[n]$ , defined as

$$x_+[n] = \mathcal{R}[\mathcal{F}^{-1}[X_+(e^{j\omega})]] \quad (4)$$

$$x_-[n] = \mathcal{R}[\mathcal{F}^{-1}[X_-(e^{j\omega})]] \quad (5)$$

where the operator  $\mathcal{R}[\cdot]$  extracts the real component of a complex signal. Real-valued EMD can then be applied to  $x_+[n]$  and  $x_-[n]$ , to give

$$x_+[n] = \sum_{i=1}^{N^+} x_i[n] + r_+[n] \quad (6)$$

$$x_-[n] = \sum_{i=-1}^{-N^-} x_i[n] + r_-[n] \quad (7)$$

where symbols  $N^+$  and  $N^-$  denote respectively the number of IMFs for the positive and the negative frequency parts,  $x_i[n]$  are the IMFs, while  $r_+[n]$  and  $r_-[n]$  represent respectively the residual signals for  $x_+[n]$  and  $x_-[n]$ . The original complex signal  $x[n]$  can then be reconstructed in terms of  $x_+[n]$  and  $x_-[n]$  as

$$x[n] = (x_+[n] + j\mathcal{H}[x_+[n]]) + (x_-[n] + j\mathcal{H}[x_-[n]])^* \quad (8)$$

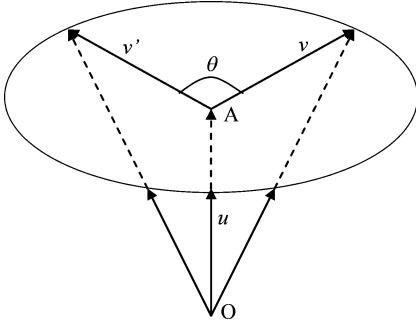


Fig. 1. Rotation of a 3D vector  $\mathbf{v} \in \mathbb{R}^3$  about line segment  $\overline{OA}$  by an angle  $\theta$ .

where  $\mathcal{H}(\cdot)$  is the Hilbert transform operator and the symbol  $(\cdot)^*$  denotes the complex conjugation operator.

For the  $i$ th complex IMF  $y_i[n]$ , defined as

$$y_i[n] = \begin{cases} x_i[n] + j\mathcal{H}[x_i[n]], & i = 1, \dots, N^+ \\ (x_i[n] + j\mathcal{H}[x_i[n]])^*, & i = -N^-, \dots, -1 \end{cases} \quad (9)$$

the original complex-valued signal  $x[n]$  can also be written as

$$x[n] = \sum_{i=-N^-, i \neq 0}^{i=N^+} y_i[n] + r[n] \quad (10)$$

where  $r[n]$  represents the trend in the data and is represented in terms of the residuals of  $x_n^+$  and  $x_n^-$  as

$$r[n] = (r_+[n] + r_-[n]) + j\mathcal{H}(r_+[n] - r_-[n]). \quad (11)$$

The so-defined complex EMD retains the generic structure of standard EMD. However, as the number of IMFs for  $x_+[n]$  and  $x_-[n]$  can in general be different, it is difficult to interpret the meaning of the so-extracted IMFs. This limits the applications in some areas, e.g., in data fusion from multiple sources [11], and this approach is not suitable for extensions to higher dimensions.

2) *Rotation-Invariant EMD (RI-EMD)*: The Rotation-Invariant EMD method [8] operates directly in  $\mathbb{C}$  and defines the extrema of a complex signal, a crucial step in envelope estimation, as points where the angle of the first derivative of the signal becomes zero. For a complex signal  $z(n) = x(n) + jy(n)$ , it can be shown that this criterion is equivalent to  $\dot{y}(n) = 0$ , that is, the extrema of the imaginary part. As it is assumed that a local maximum is always followed by a local minimum, these sets can be interchanged. The spline interpolation is then performed on both the components separately to obtain complex-valued envelopes, which are then averaged to obtain the local mean. This method yields a single set of complex-valued IMFs, and the ambiguity at the zero frequency within complex EMD is avoided due to the direct operation in  $\mathbb{C}$ . However, since this method uses the extrema of only the imaginary component of a bivariate signal to calculate the local mean of the envelopes, its accuracy may be compromised.

3) *Bivariate EMD*: The bivariate EMD algorithm [9] calculates the local mean envelopes based on the extrema of both (real and imaginary) components of a complex signal, yielding more accurate estimates than RI-EMD. It projects the bivariate

signal in  $k$  different directions and obtains the corresponding envelopes by interpolating the extrema of projected signals via component-wise spline interpolation. The method extends the intuitive notion of ‘‘oscillations’’ in the real-valued EMD to its 2D counterpart ‘‘rotations,’’ thus yielding bivariate intrinsic mode functions. The bivariate EMD method, therefore, effectively sifts rapidly rotating signal components from the slowly rotating ones. In Algorithm 2, the steps to calculate the local mean of the complex signal using bivariate EMD are given.

#### Algorithm 2 Bivariate Extension of EMD

- 1: Obtain  $K$  signal projections, denoted by  $\{p_{\theta_k}\}_{k=1}^K$ , by projecting the complex signal  $z(t)$ , by means of a unit amplitude complex number  $e^{-j\theta_k}$ , in the direction of  $\theta_k$ , as

$$p_{\theta_k} = \Re(e^{-j\theta_k} z(t)), \quad k = 1, \dots, K \quad (12)$$

where  $\Re(\cdot)$  denotes the real part of a complex number, and  $\theta_k = 2k\pi/K$ ;

- 2: Find the locations  $\{t_j^k\}_{k=1}^K$  corresponding to the maxima of  $\{p_{\theta_k}\}_{k=1}^K$ .
- 3: Interpolate (using spline interpolation) between the maxima  $[t_j^k, z(t_j^k)]$ , to obtain the envelope curves  $\{e_{\theta_k}\}_{k=1}^K$ .
- 4: Calculate the mean,  $m(t)$ , of all the envelope curves.
- 5: Subtract  $m(t)$  from the input signal  $z(t)$  to yield an ‘‘oscillatory’’ component, that is,  $d(t) = z(t) - m(t)$ .

Similarly to real-valued EMD, if  $d(t)$  meets the stoppage criterion for bivariate IMFs, then the process is reapplied to  $z(t) - d(t)$ ; otherwise, it is applied to  $d(t)$ . The stoppage criterion for the bivariate IMF is similar to that employed in [23].

Notice from RI-EMD and bivariate EMD that the critical point in 2D extensions of EMD is to find the locations of local minima and maxima. RI-EMD uses projections in only two directions to find the extrema, whereas bivariate EMD uses projections in multiple directions by projecting the signal in 2D (complex) plane using a unit amplitude complex exponential. The issue of finding the extrema of a signal is even more crucial when operating in more than two dimensions. We next propose an extension of EMD for trivariate signals, whereby the extrema are found by projecting the input signal in multiple directions in three dimensions via a quaternion rotation framework.

### III. QUATERNION ALGEBRA

A quaternion  $q \in \mathbb{H}$  is defined as  $q = s + xi + yj + z\kappa$ , where  $s, x, y,$  and  $z$  are real numbers and  $i, j,$  and  $\kappa$  are the unit vectors along the three vector dimensions [16]. Addition of quaternions is defined as

$$\begin{aligned} q_0 + q_1 &= (s_0 + x_0i + y_0j + z_0\kappa) \\ &\quad + (s_1 + x_1i + y_1j + z_1\kappa) \\ &= (s_0 + s_1) + (x_0 + x_1)i \\ &\quad + (y_0 + y_1)j + (z_0 + z_1)\kappa. \end{aligned} \quad (13)$$

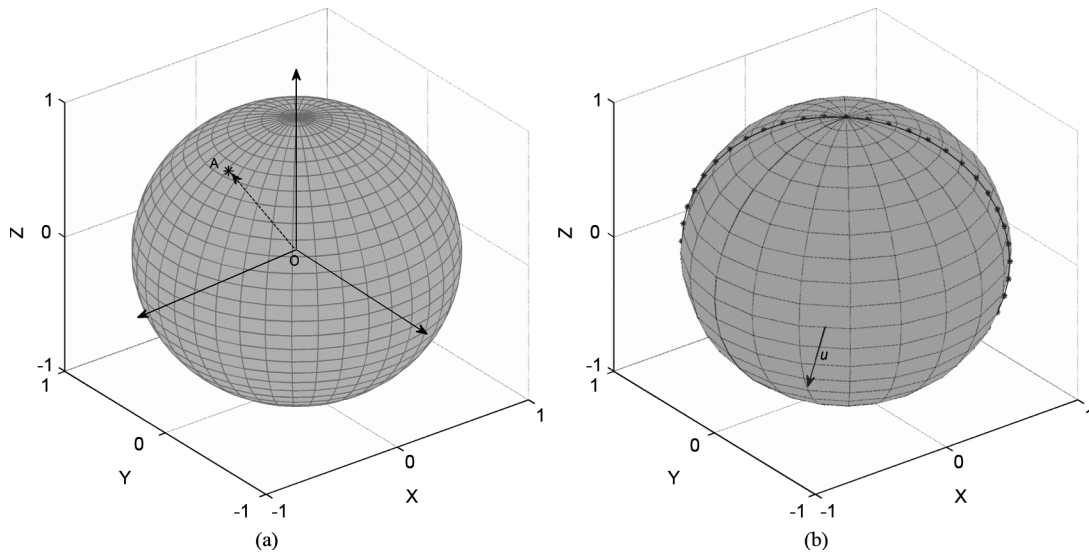


Fig. 2. Projections for trivariate signals. (a) The direction vector  $OA$  in 3D space, which has unit norm, can also be represented by a point on the surface of a unit sphere. (b) Multiple direction vectors represented by points on a longitude line. Projections of the input signal are taken by rotation about the vector  $u$ . To encompass the whole 3D space, direction vectors on multiple longitude lines should be considered.

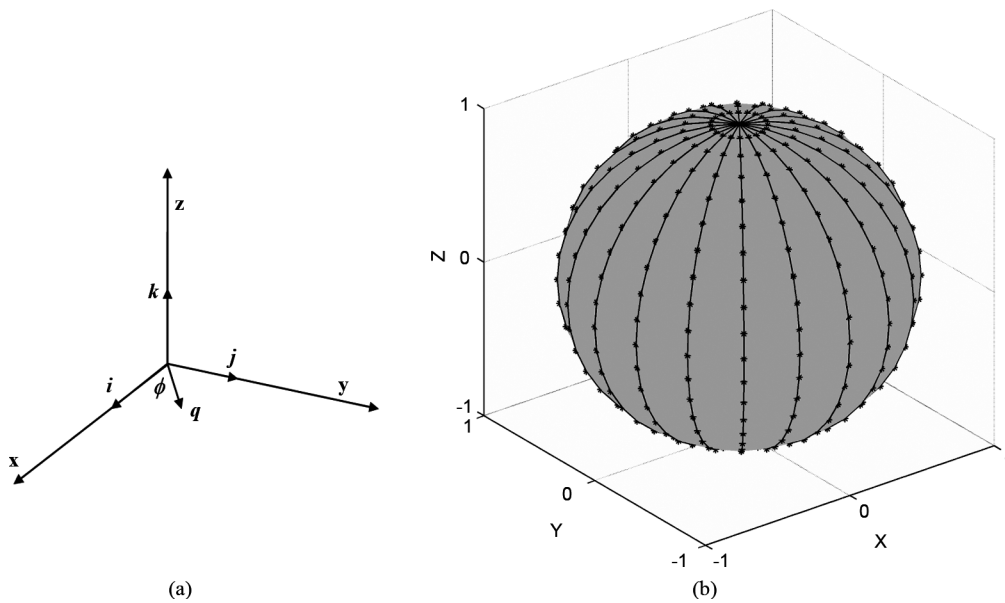


Fig. 3. Generating multiple direction vectors in a 3D space. (a) Choices of rotation axes to obtain projections along multiple directions in a 3D space. For projections along longitudinal lines on a sphere, multiple axes represented by a set of vectors  $q$  are chosen in the  $xy$  plane, with angle  $\phi$  taken with respect to  $+x$ -axis. (b) Points on multiple longitudinal lines on a sphere, representing directions along which projections of the input signal can be taken by rotating the input signal along rotation axes represented by a set of unit quaternions  $q$ .

and the unit elements  $i, j,$  and  $\kappa$  are related as

$$\begin{aligned}
 ij\kappa &= i^2 = j^2 = \kappa^2 = -1 \\
 ij &= \kappa = -ji \\
 j\kappa &= i = -\kappa j \\
 \kappa i &= j = -i\kappa.
 \end{aligned}
 \tag{14}$$

From (13) and (14), observe that the quaternion multiplication is not commutative. Subtraction of quaternions can be described as the addition and multiplication by  $-1$ .

The conjugate of a quaternion  $q$  is defined as

$$q^* = (s + xi + yj + z\kappa)^* = s - xi - yj - z\kappa \tag{15}$$

whereas the norm of the quaternion is given by

$$\|q\| = \|s + xi + yj + z\kappa\| = \sqrt{s^2 + x^2 + y^2 + z^2}. \tag{16}$$

Of special interest for this work is the so-called unit quaternion, which has a unit norm and can be written as

$$q = \cos \theta + \text{usin } \theta \tag{17}$$

where  $\mathbf{u}$  is a 3D vector of unit length. A unit quaternion also has an exponential form given by

$$e^{\mathbf{u}\theta} = \cos \theta + \mathbf{u} \sin \theta. \quad (18)$$

The above equation can be seen as the generalization of Euler's identity for complex numbers and represents the rotation of a vector by an angle  $2\theta$  about a 3D unit vector  $\mathbf{u}$ . Fig. 1 illustrates the rotation of a vector  $\mathbf{v}$  by an angle  $\theta$  about the line segment  $\overline{OA}$ . The direction of  $\overline{OA}$  is specified by a 3D unit vector  $\mathbf{u} \in \mathbb{R}^3$ , and the rotated vector is represented by  $\mathbf{v}'$ , that is

$$\mathbf{v}' = q\mathbf{v}q^* = e^{\mathbf{u}\theta/2}\mathbf{v}(e^{\mathbf{u}\theta/2})^*. \quad (19)$$

Note that both the quaternion  $q$  and  $-q$  represent the same rotation of a 3D vector  $\mathbf{v}$ .

#### IV. TRIVARIATE EMPIRICAL MODE DECOMPOSITION

A major challenge in extending standard EMD to multivariate signals is to find an accurate method for calculating the local mean since the concept of extrema cannot always be rigorously defined for multivariate signals. In the bivariate extension of EMD, the local mean of an input signal is calculated by taking projections of a bivariate signal in multiple directions. The direction vectors, along which signal projections are taken, are uniformly distributed in the complex plane. The maxima of the resulting projections are interpolated via complex splines to obtain envelope curves, which are then averaged to yield an approximation of the local mean.

To extend this idea to trivariate signals, we need to obtain signal projections in multiple directions in 3D spaces. The extrema of these signal projections can then be interpolated using a component-wise spline interpolation, yielding 3D pure quaternion-valued envelope curves. The use of component-wise spline interpolation for pure quaternion signals represents an extension of the concept of "complex splines," employed in RI-EMD and bivariate EMD. The resulting "quaternion-valued envelopes" are then averaged to obtain an estimate of the local mean of a 3D signal.

To obtain signal projections along different directions, multiple direction vectors are chosen in a 3D space. The direction vectors can be conveniently represented by points on the surface of a unit sphere. Each point on the surface corresponds to the terminal point of a direction vector drawn from the center of the sphere; one such point and its associated direction vector is shown in Fig. 2(a). To generate a set of multiple direction vectors in a 3D space, we generate a lattice by taking equidistant points on multiple longitudinal lines on the sphere, obtaining so called "equi-longitudinal lines." The projection of the input signal along these points (direction vectors) on an equi-longitudinal line can then be obtained by rotating the input signal along a rotation axis in the  $xy$  plane and mapping it on the  $z$ -axis. Multiple points (direction vectors) on a single longitudinal line, corresponding to rotation axis  $u$ , along which the projections can be taken are shown in Fig. 2(b). Every rotation in three dimensions can be treated as a rotation about an axis by a given angle. Thus, a unit quaternion, which gives an efficient and convenient

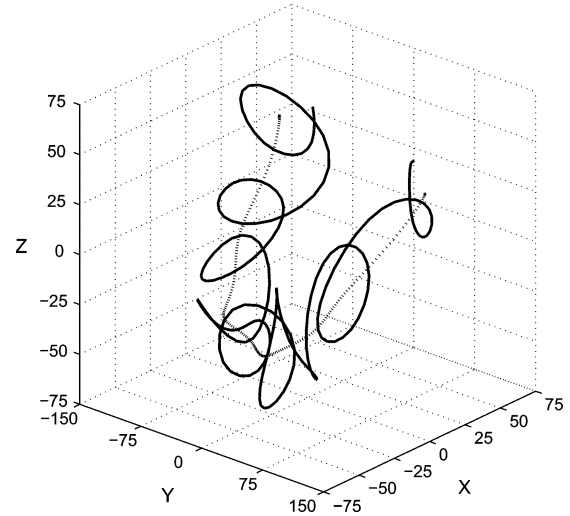


Fig. 4. Local mean (dotted line) calculated for a trivariate signal (solid line) using (22) in Algorithm 3.

mathematical notion for rotation using an angle-axis representation, is a natural choice for performing 3D rotations.

To take projections along direction vectors spanning the whole 3D space, we employ multiple rotation axes along the  $xy$  plane. By rotating the input signal along these axes, we can obtain signal projections along the directions corresponding to multiple equi-longitudinal lines on the surface of the sphere, as shown in Fig. 3(b). Since rotation axes are 3D vectors, they can also be represented by a set of unit quaternions  $\mathbf{q}$  in the  $xy$  plane, under an angle  $\phi$  to the  $x$ -axis as shown in Fig. 3(a). Rotation axes, represented by a vector of quaternions  $\mathbf{q}$ , can therefore be expressed as

$$\mathbf{q} = 0 + \cos(\phi)i + \sin(\phi)j + 0k. \quad (20)$$

Since a trivariate signal can also be represented as a pure quaternion  $x(t)$ , the projections of the input signal along multiple direction vectors on the sphere [Fig. 3(b)] can be calculated by rotating the input signal [using (19)] about a set of vectors  $q$  and taking its projection along the  $z$ -axis ( $\kappa$ ), using

$$p_\theta^\phi = e^{\mathbf{q}\theta}x(t)(e^{\mathbf{q}\theta})^* \cdot \kappa \quad (21)$$

where symbol " $\cdot$ " denotes the dot product. To calculate the envelopes in multiple directions, angles  $\phi$  and  $\theta$  can be selected to respectively have  $N$  and  $K$  values between 0 to  $\pi$ . The range of  $\pi$  is necessary since both  $q$  and  $-q$  give projections in the same direction, and also from (19), the application of a unit quaternion  $q$  represents rotation by an angle  $2\theta$ .

While projections of the input signal on points (direction vectors) along equi-longitudinal lines on a sphere provide reasonable solution, it can be noticed from Fig. 3(b) that there is greater concentration of points close to the North and South pole of the sphere, and therefore, the points close to the poles are given more "weight" in the calculation of the local mean signal. As a result, the method would not be strictly invariant to 3D rotations, although it spans the whole 3D space for a large number

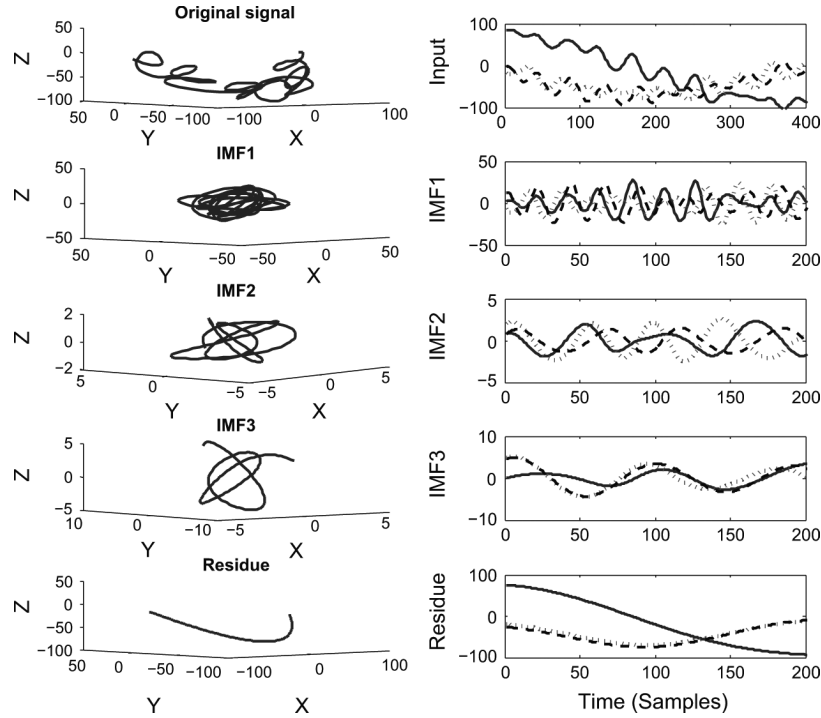


Fig. 5. A trivariate signal and its decomposition obtained using the proposed method. 3D plots of the input trivariate signal followed by the IMFs are shown on the left. Time plots of the three components of the trivariate signal and their decomposition are also shown (X: dotted line, Y: solid line, Z: dashed line).

of points and hence provides a satisfactory solution.<sup>1</sup> The extension of EMD for pure quaternion signals is summarized in Algorithm 3.

#### Algorithm 3 Trivariate Extension of EMD

- 1: Calculate projections, denoted by  $p_{\theta_k}^{\phi_n}(t)$ , of a trivariate quaternion signal  $x(t)$  using (21), where  $\theta_k = k\pi/K$  for  $k = 1, \dots, K$ , and  $\phi_n = n\pi/N$  for  $n = 1, \dots, N$ ;
- 2: Find the time instants  $\{(t_k^n)_i\}$  corresponding to the maxima of  $p_{\theta_k}^{\phi_n}(t)$ , for all values of  $k$  and  $n$ ;
- 3: Interpolate  $[(t_k^n)_i, x((t_k^n)_i)]$  to obtain quaternion envelope curves  $e_{\theta_k}^{\phi_n}$ , for all  $k$  and  $n$ ;
- 4: Compute the mean  $m(t)$  of all the envelope curves using:

$$m(t) = \frac{1}{KN} \sum_{k=1}^K \sum_{n=1}^N e_{\theta_k}^{\phi_n}. \quad (22)$$

- 5: Extract the “detail”  $d(t)$  using  $d(t) = x(t) - m(t)$ .  
If the “detail”  $d(t)$  fulfills the stoppage criterion for a quaternion-valued IMF, then the above procedure is applied to  $x(t) - d(t)$ , otherwise it is applied to  $d(t)$ .

The stoppage criterion for quaternion-valued IMF is similar to that proposed in [23], the difference being that the condition

<sup>1</sup>To make the method asymptotically rotation-invariant, an average of envelopes  $e_{\theta_k}^{\phi_n}$  can be taken on the surface of the sphere using  $m(t) = 1/4\pi \int_S e_{\theta_k}^{\phi_n} d\Omega$ , where  $d\Omega$  corresponds to the differential solid angle on sphere  $S$ . The mean envelope can then be calculated by using  $m(t) \approx \pi/2KN \sum_{k=1}^K \sum_{n=1}^N e_{\theta_k}^{\phi_n} |\sin 2\theta_k|$ , where the weighting factor  $|\sin 2\theta_k|$  compensates for the higher density of the point set by giving smaller weights to envelopes near poles; this scheme, however, has problems for smaller values of  $K$  and  $N$ .

for equality of the number of extrema and zero crossings is not imposed since extrema cannot be properly defined for quaternion-valued IMFs. Fig. 4 shows the results of employing the mean envelope (22) in Algorithm 3 for the calculation of the local mean of a trivariate signal, using  $K = 6$  and  $N = 6$ . Notice that the local mean correctly tracks the dynamics of the signal.

The original EMD method aims to extract the oscillatory components embedded in the data, called “intrinsic mode functions.” The bivariate IMFs, obtained from bivariate extensions of EMD, extend the notion of oscillation in two dimensions to extract 2D rotational modes. Similarly, the proposed method is designed to obtain rotational components in 3D spaces, if present, within the trivariate signal. The mean envelope, which defines the overall trend in the signal, is considered as a slowly rotating signal and is subtracted from the input signal until the “detail” (fast rotating component) is extracted. Similarly to real-valued EMD and its bivariate extensions, the algorithm can also decompose signals carrying no physically meaningful rotating components, e.g., trivariate white noise signal.

For illustration, the decomposition of a trivariate signal<sup>2</sup> is performed using the proposed trivariate extension of EMD, and the results are shown in Fig. 5. The different 3D rotating modes of the input trivariate signal are extracted, whereby the lower index IMFs contain higher frequency 3D rotations and the higher index IMFs represent lower frequency rotating modes, as shown in Fig. 5. The residue signal does not contain any 3D rotating components. Time plots of the individual components of input trivariate signal and their respective decomposition

<sup>2</sup>The signal represents the 3D orientation data generated by hand movements in a Tai Chi sequence, with a synthetically added mode for illustration purpose. The data was captured using an inertial 3D sensor.

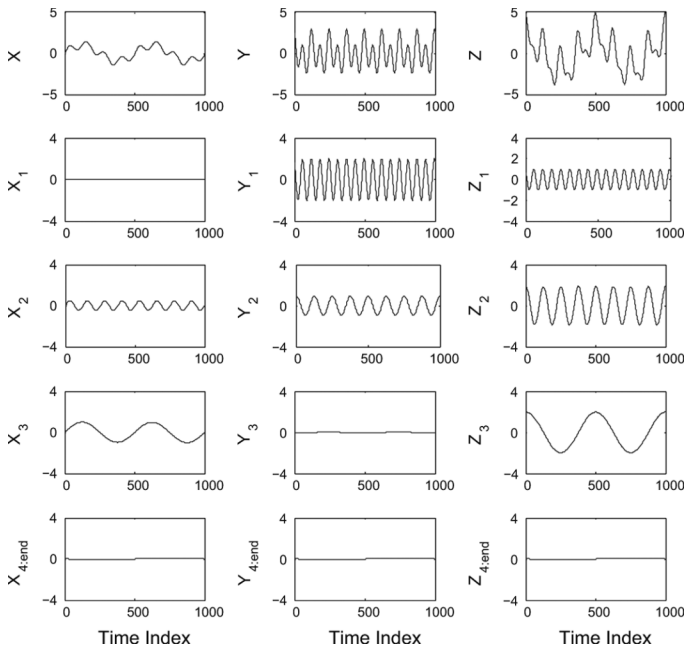


Fig. 6. Decomposition of a synthetic quaternion signal, with multiple frequency modes, via the proposed trivariate EMD algorithm. Each quaternion-valued IMF carries a single frequency mode, thereby facilitating the alignment of common modes within different components of a trivariate signal.

(IMFs) are also shown in Fig. 5. The decomposition of individual components exhibits the mode alignment property, whereby common frequency modes in different input components are aligned in single IMF. This property is further demonstrated in the next section.

### V. COMMON SCALE/MODE ALIGNMENT USING QUATERNION-VALUED IMFs

We now perform an analysis of quaternion-valued IMFs to demonstrate their ability to align “common scales” present within the data. Complex extensions of EMD, exhibiting similar mode aligning property have recently found application in data fusion [11]. The alignment of oscillatory modes of the input trivariate signal represented by pure quaternion IMFs allows to combine information of same nature from different IMFs and, hence, facilitates the fusion of information from up to three sources.

To illustrate the mode alignment property of the proposed method, pure quaternion signal was constructed from a set of three sinusoidal signals shown in the top row of Fig. 6 (denoted by  $X$ ,  $Y$ , and  $Z$ ). One sinusoid was made common to all the components ( $X$ ,  $Y$ , and  $Z$ ), whereas the remaining two sinusoidal components were used so that the resulting signal had a common frequency mode in both  $Y$  and  $Z$  and  $X$  and  $Z$ . The trivariate EMD algorithm was then applied to the resulting quaternion signal yielding multiple quaternion-valued IMFs, as shown in Fig. 6. Observe that the sinusoid common to all the components of the input is the second IMF, whereas the remaining two frequency modes are present in IMFs one and three. Such mode alignment cannot be achieved by using the real-valued EMD component-wise, as it generally does not yield the same number of IMFs per component.

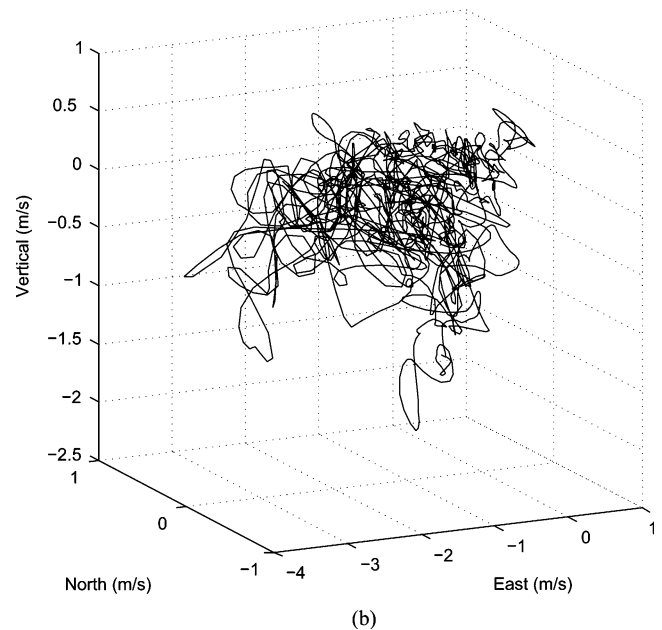
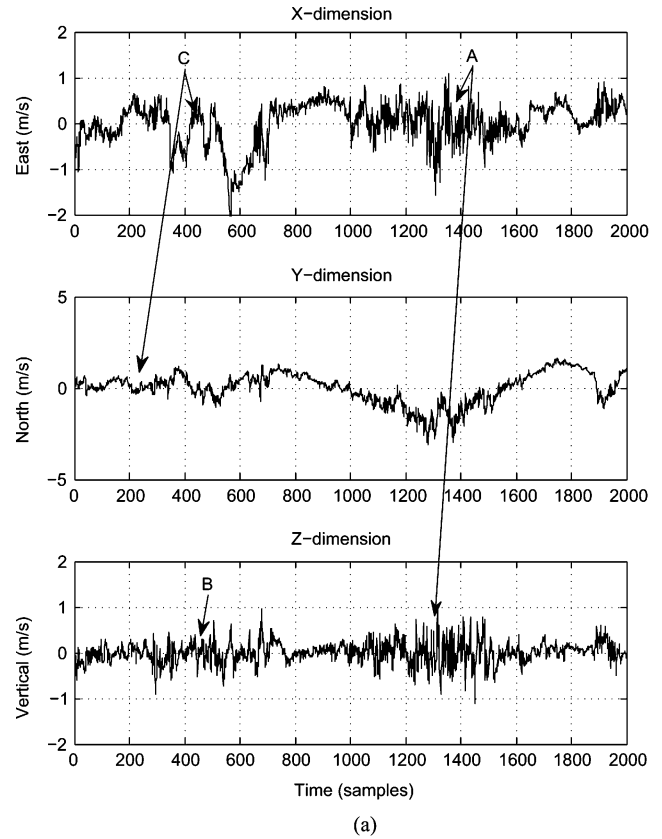


Fig. 7. A 3D wind signal represented as a pure quaternion. (a) Wind speed in the east-west ( $X$ ), north-south ( $Y$ ), and the vertical ( $Z$ ) direction. Wind regime with high dynamics is denoted by “A.” The regimes with mild and low dynamics are denoted by symbols “B” and “C”. (b) The 3D local mean of the wind signal from (a), obtained by applying the mean-envelope detection method, given in Algorithm 3.

### VI. SIMULATION RESULTS

Simulations were conducted on synthetic signals and on real-world 3D wind data. For all the signals, the number of directions used to calculate the mean envelope was set to  $K = 16$  and  $N = 16$ .

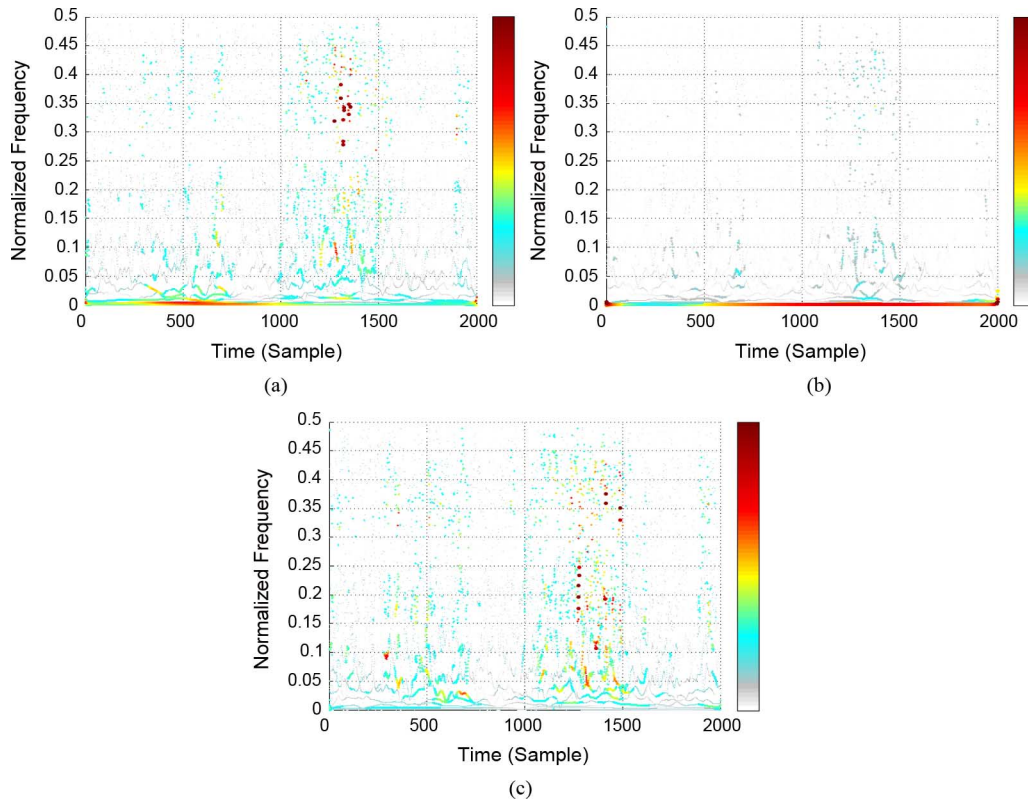


Fig. 8. Hilbert–Huang spectra of IMFs of wind signal components in (a) East-West direction ( $X$ ), (b) North-South direction ( $Y$ ), and (c) vertical direction ( $Z$ ).

### A. Time-Frequency Analysis

In the first set of simulations, an application of the proposed algorithm to time-frequency analysis of a 3D wind signal was conducted. Time-frequency analysis of wind can provide important information in order to identify critical episodes of wind behavior, including gusts and turbulence. Traditional Fourier-based spectral methods are bound to fail in those cases due to the nonstationarity of the wind signal. The East, North, and Upward velocity, shown in Fig. 7(a), were represented as  $X$ ,  $Y$ , and  $Z$  components of the pure quaternion signal  $x(t)$ , that is

$$x(t) = 0 + X_i + Y_j + Z_k. \quad (23)$$

Fig. 7(b) shows the trend in the wind dynamics visualized through the mean envelope of trivariate wind signal. Fig. 7(a) also shows segments of the wind signal with different dynamics, denoted respectively by “A,” “B,” and “C.” A wind regime with high dynamic (“A”) exhibits larger changes in wind speed in relatively small time intervals and should contain high-frequency components in the corresponding Hilbert–Huang spectrum, while medium (“B”) and lower dynamic (“C”) regimes are expected to contain predominantly lower frequency components. This is illustrated in Fig. 8, which shows the Hilbert–Huang spectra of the wind signal from Fig. 7. The spectrum of the North wind speed component [see Fig. 8(b)], belonging to the low-dynamics wind regime, was mostly dominated by low frequency components. Wind regimes denoted by “C” had mostly lower frequency components in the corresponding frequency spectrum, for instance, around sample 500 in Fig. 8(a). In

contrast, for wind regimes with high dynamics, the spectrum had more pronounced magnitudes at higher frequencies. The high variations in the wind speed in the Upward and the East components, observed at samples 1200–1400, can be clearly observed in the corresponding spectra in Fig. 8(a) and (c), showing the power is spread over a wide range of frequencies, exhibiting several bursts at high frequency.

### B. 3D Rotational Mode Extraction

We shall now demonstrate the ability of the proposed algorithm to extract the 3D rotational modes from the signal. This may be useful in applications where phase relation between signal components is of relevance. For illustration, we use a synthetic Hodgkin–Huxley-based neuron model [24] to generate regular spikes. A known delay is added to the original signal to generate multiple channel components, and the noise is then added channel-wise. The three channels are then combined to form a synthetic quaternion signal using (23), as shown in Fig. 9(a).

Fig. 9(b) shows the IMFs extracted after applying the trivariate EMD method to the input signal [shown in Fig. 9(a)]. The first few IMFs, represented by large-scale non-rotating modes in Fig. 9(b), correspond to the high-frequency noise embedded in the data. The most dominant rotational mode (quaternion IMF) corresponding to the original spike signal was the fourth IMF in our simulation, also illustrating the mode alignment property of quaternion IMFs. Fig. 10 shows 3D plots of the input signal [Fig. 10(a)] and the relevant IMF [Fig. 10(b)]. The 3D rotating modes are expected to give information regarding the phase relationship between the components of the

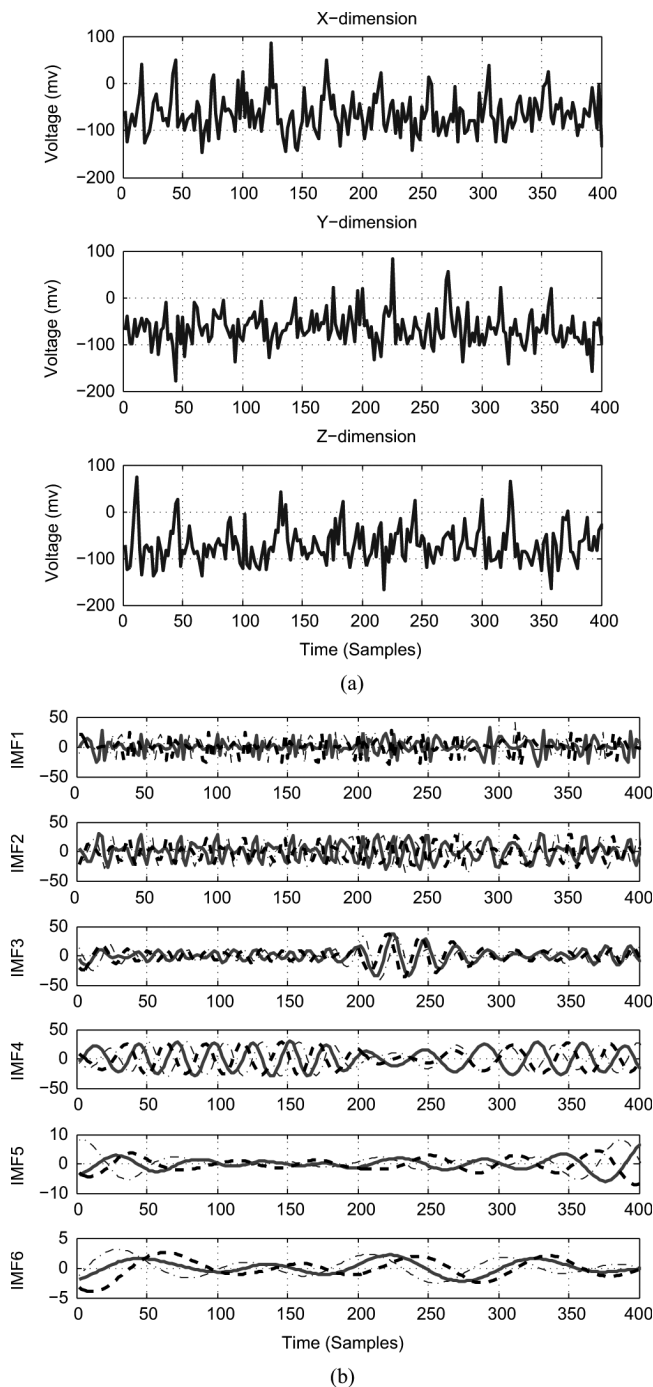


Fig. 9. A synthetic spiking cortical neuron signal with added noise, together with its delayed versions. (a) The three components are combined to form a pure quaternion signal. (b) The components of the first six quaternion IMFs (X: dotted line, Y: solid line, Z: dashed line) obtained by decomposing the signal in (a).

multivariate signals and may be used in applications requiring phase synchronization.

VII. CONCLUSION

We have proposed an extension of empirical mode decomposition (EMD) in order to make it suitable for the processing of trivariate signals. The trivariate signal is represented as a pure quaternion, and the rotation property of unit quaternions

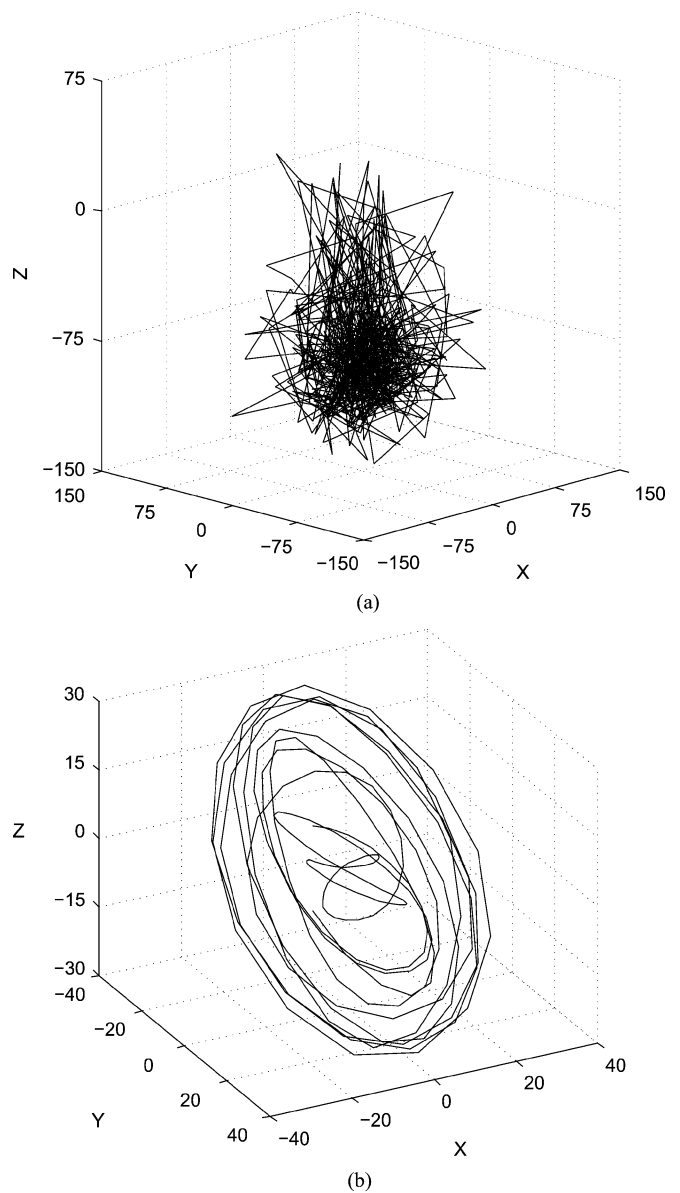


Fig. 10. The synthetic trivariate spiking neuron signal and the relevant rotational mode. (a) 3D plot of the input signal (b) 3D plot of the relevant rotational mode.

is employed to obtain multiple projections of the input signal along “equi-longitudinal” lines on the sphere, thus offering a compact and convenient mathematical representation. The method extracts the 3D rotating components of the input trivariate signal and also generates common oscillatory modes, facilitating the fusion of information from multiple sources. Simulations on real-world 3D data have also illustrated the potential of the proposed method in the time-frequency analysis of trivariate signals.

ACKNOWLEDGMENT

Gill Instruments Ltd. have provided WindMaster, a 3D ultrasonic anemometer, used for wind readings. The authors also wish to thank the anonymous reviewers for their insightful comments and help towards the final version of the manuscript.

## REFERENCES

- [1] N. Huang, Z. Shen, S. Long, M. Wu, H. Shih, Q. Zheng, N. Yen, C. Tung, and H. Liu, "The empirical mode decomposition and Hilbert spectrum for non-linear and non-stationary time series analysis," *Proc. Royal Soc. A*, vol. 454, pp. 903–995, 1998.
- [2] N. E. Huang and S. Shen, *Hilbert-Huang Transform and its Applications*. Singapore: World Scientific, 2005.
- [3] N. E. Huang and Z. Wu, "A review on Hilbert-Huang transform: Method and its applications to geophysical studies," *Rev. Geophys.*, vol. 46, 2008.
- [4] D. J. Duffy, "The application of Hilbert-Huang transforms to meteorological datasets," *J. Atmos. Ocean. Technol.*, vol. 21, no. 4, pp. 599–611, 2004.
- [5] Z. Wu and N. E. Huang, "Ensemble empirical mode decomposition: A noise-assisted data analysis method," *Adv. Adaptive Data Anal.*, vol. 1, pp. 1–41, 2009.
- [6] D. P. Mandic and V. S. L. Goh, *Complex Valued Non-Linear Adaptive Filters: Noncircularity, Widely Linear Neural Models*. Hoboken, NJ: Wiley, 2009.
- [7] T. Tanaka and D. P. Mandic, "Complex empirical mode decomposition," *IEEE Signal Process. Lett.*, vol. 14, no. 2, pp. 101–104, Feb. 2006.
- [8] M. U. Altaf, T. Gautama, T. Tanaka, and D. P. Mandic, "Rotation invariant complex empirical mode decomposition," in *Proc. IEEE Int. Conf. Acoust., Speech, Signal Process.*, 2007, vol. 3, pp. 1009–1112.
- [9] G. Rilling, P. Flandrin, P. Goncalves, and J. M. Lilly, "Bivariate empirical mode decomposition," *IEEE Signal Process. Lett.*, vol. 14, no. 12, pp. 936–939, Dec. 2007.
- [10] *Signal Processing Techniques for Knowledge Extraction and Information Fusion*, D. P. Mandic, M. Golz, A. Kuh, D. Obradovic, and T. Tanaka, Eds. New York: Springer, 2008.
- [11] D. Looney and D. P. Mandic, "Multi-scale image fusion using complex extensions of EMD," *IEEE Trans. Signal Process.*, vol. 57, no. 4, pp. 1626–1630, Apr. 2009.
- [12] J. C. Nunes, Y. Bouaoune, E. Dellechelle, O. Niang, and P. Bunel, "Image analysis by bidimensional empirical mode decomposition," *Image Vision Comput.*, vol. 21, pp. 1019–1026, 2003.
- [13] A. Linderhed, "Compression by image empirical mode decomposition," in *Proc. IEEE Int. Conf. Image Process.*, 2006, vol. 1, pp. 553–556.
- [14] W. Hamilton, "Elements of quaternions," Longmans, Green and Co., 1899.
- [15] D. Eberly, "Quaternion algebra and calculus," Geometric Tools, LLC, 1999.
- [16] E. B. Dam, M. Koch, and M. Lillholm, "Quaternions, interpolation and animation," Univ. Copenhagen, Denmark, 1998.
- [17] A. J. Hanson, *Visualizing Quaternions*. Amsterdam, The Netherlands: Elsevier, 2006.
- [18] C. Cheong-Took and D. P. Mandic, "The quaternion LMS algorithm for adaptive filtering of hypercomplex real world processes," *IEEE Trans. Signal Process.*, vol. 57, no. 4, pp. 1316–1327, Apr. 2009.
- [19] N. L. Bihan and J. Mars, "Singular value decomposition of quaternion matrices: A new tool for vector-sensor signal processing," *Signal Process.*, vol. 84, no. 7, pp. 1177–1199, 2004.
- [20] A. M. Sabatini, "Quaternion-based strap-down integration method for applications of inertial sensing to gait analysis," *Med. Biol. Eng. Comput.*, vol. 43, pp. 94–101, 2005.
- [21] D. Biamino, G. Cannata, M. Maaggiali, and A. Piazza, "MAC-EYE: A tendon driven fully embedded robot eye," in *Proc. IEEE-RAS Int. Conf. Humanoid Robots*, 2005, pp. 62–67.
- [22] N. Huang, M. Wu, S. Long, S. Shen, W. Qu, P. Gloersen, and K. Fan, "A confidence limit for the empirical mode decomposition and Hilbert spectral analysis," *Proc. Royal Soc. London*, vol. 459, pp. 2317–2345, 2003.
- [23] G. Rilling, P. Flandrin, and P. Goncalves, "On empirical mode decomposition and its algorithms," in *Proc. IEEE-EURASIP Workshop NSIP*, 2003.
- [24] E. M. Izhikevich, "Simple model of spiking neurons," *IEEE Trans. Neural Netw.*, vol. 14, no. 6, pp. 1569–1572, Nov. 2003.



**Naveed ur Rehman** (S'09) received the B.Eng. degree in electrical engineering from National University of Sciences and Technology, Islamabad, Pakistan, in 2004. Currently, he is pursuing the Ph.D. degree in adaptive nonlinear signal processing at Imperial College London, London, U.K.

His post-graduate studies are funded by a prestigious scholarship from Higher Education Commission, Government of Pakistan. His research interests are mainly in the areas of time-frequency analysis and nonlinear signal processing.



**Danilo P. Mandic** (M'99–SM'03) is a Reader in Signal Processing at Imperial College London. He has been working in the area of nonlinear adaptive signal processing and nonlinear dynamics. His publication record includes two research monographs titled *Recurrent Neural Networks for Prediction* (1st ed., Aug. 2001) and *Complex Valued Nonlinear Adaptive Filters: Noncircularity, Widely Linear and Neural Models* (1st ed., Wiley, Apr. 2009), an edited book titled *Signal Processing for Information Fusion* (Springer, 2008) and more than 200 publications on signal and image processing. He has been a Guest Professor at K.U. Leuven Belgium, TUAT Tokyo, Japan, and Westminster University, U.K., and a Frontier Researcher in RIKEN Japan.

Dr. Mandic has been a Member of the IEEE Technical Committee on Machine Learning for Signal Processing, Associate Editor for the IEEE TRANSACTIONS ON CIRCUITS AND SYSTEMS II, IEEE TRANSACTIONS ON SIGNAL PROCESSING, IEEE TRANSACTIONS ON NEURAL NETWORKS, and the *International Journal of Mathematical Modelling and Algorithms*. He has produced award winning papers and products resulting from his collaboration with Industry. He is a Member of the London Mathematical Society.